International Journal of Gas Turbine, Propulsion and Power Systems
June 2012, Volume 4, Number 2

Single Entry Mixed Flow Turbine Performance Prediction With 1-D Gas Dynamic Code Coupled With Mean Line Model

M. S. Chiong[1], S. Rajoo[1]*, A. Romagnoli[2] and R. F. Martinez-Botas[2]

[1]Transportation Research Alliance,Universiti Teknologi Malaysia, 81310 Johor, Malaysia
[2]Dept of Mechanical Engineering, Imperial College London, SW7 2AZ London, UK

ABSTRACT

It is a well known fact that turbocharger works with pulsating exhaust flow in its entire operating life, hence the need to predict unsteady performance. This paper presents the unsteady performance prediction resultof a single entry nozzleless mixed flow turbine under steady flow and 60 Hz pulsating flow at 43.0 rps/$\sqrt{K}$ operating speed. The modeling method coupled one-dimensional gas dynamic modelwith a mean-line model to predict the turbine efficiency by appropriate losses consideration. The coupled method assumes that the turbine volute has a large volume and length, so that unsteadiness effect of the pulsating flow is significant while the rotor is assumed to behave quasi-steadily. A pressure drop boundary is used to simulate pressure drop across the turbine volute. The coupled method was validated with the experimentally measured steady state results of the same turbine. Experimentally measured total conditions of the flow were used as inlet conditions for the model during unsteady analysis. The predicted isentropic power averaged results show convincing match with the experimental data. This will set forward a systematic approach for engine designers to evaluate turbine performance beyond what will be normally provided by turbocharger manufacturers, which is the steady state map.

Keyword: Turbine, performance prediction, one-dimensional gas dynamic model, mean-line model, losses

Presented at International Gas Turbine Congress 2011 Osaka, November 13-18, Osaka, Japan, IGTC2011-0158
Review completed March 30, 2012

INTRODUCTION

Turbocharging technology is believed to play a crucial role in the engine downsizing development towards reducing green house emissions. In a case study conducted by Drescher [1], it was found that engine downsizing may contribute up to approximately 24% of the overall achievable fuel efficiency optimization. Due to the lower cost increment per unit CO_2 reduction, internal combustion engine is forecasted to be the main powertrain source at least for the following two decades [2]. Computational turbine modeling is a powerful analysis tool yet much cheaper option in conjunction with the development of turbocharging technology, such as in the engine-turbocharger matching and optimizing exhaust system. In this paper, a precise modeling method for unsteady turbine performance prediction, which subsequently able to be used in engine model will be presented.

Mean Line Model

A mean line model calculates the turbine performance along the mean path line of gas flow through a turbine. Turbine is divided into sections for calculation where losses are assumed to take place. Along the turbine volute, the mean path line of gas flow is essentially line connecting the centroid of volute cross section. Since the calculation is only performed one-dimensionally, gas flow is assumed to enter into rotor at one nominal point that is at 180° azimuth angle. This location is chosen based on the phase shifting study of instantaneous turbine flow properties under pulsating flow shown by Szymko [3]. Mean flow path through turbine rotor is assumed to lie on the meridional plane at 180° azimuth angle. The flow path throughout the turbine is illustrated in Fig 1.

NOMENCLATURE

A, F	Cross-sectional area	$[m^2]$
C, u	Velocity, absolute velocity	$[\frac{m}{s}]$
$\mathbf{C}$	Vector of source term	
C_p	Constant pressure specific heat	
e	Internal energy	$[J]$
f	Frequency	$[Hz]$
$\mathbf{F}(\mathbf{W})$	Vector in x-direction	
G	$\frac{1}{2}u\|u\|f\frac{4}{D}$	
H	Height	$[m]$
h	Specific enthalpy	$[\frac{J}{kg}]$
i	Incidence angle	$[rad]$
K	Loss coefficient	
L	Loss	
$\dot{m}$	Mass flow rate	$[\frac{kg}{s}]$
P	Pressure	$[Pa]$
q	Heat transfer rate per unit mass	$[\frac{J}{kg \cdot s}]$
r	Radius	$[m]$
T	Temperature	$[K]$
t	Time	$[s]$
U	Rotor velocity	$[\frac{m}{s}]$
$\dot{W}$	Work	$[\frac{J}{s}]$
W	Relative velocity	$[\frac{m}{s}]$
$\mathbf{W}$	Vector of convection fluxes	
x	Distance in x-direction	$[m]$
Z	Blade number	
α	Absolute flow angle	$[rad]$
β	Relative flow angle	$[rad]$
η	Efficiency	
θ	Tangential	
μ	Viscosity	$[\frac{kg}{m \cdot s}]$
ρ	Density	$[\frac{kg}{m^3}]$

Subscripts

0	Total state
1	Station 1: Inlet to turbine
2	Station 2: Upstream to rotor
23	Station 2 to 3
3	Station 3: Downstream to rotor
4	Station 4: Exit from turbine
avg	Average
b	Blade
cl	Clearance
df	Disc friction
hub	Hub side
in	Inlet
inc	Incidence
is	Isentropic
m	Meridional
opt	Optimum
out	Outlet
p	Passage
tip	Tip or shroud side

Due to the simplification of gas flow path through the turbine, it is necessary to take into account the flow losses in the form of empirical coefficient. A nozzleless turbine is assumed to consist of four stations, i.e. inlet to turbine, upstream to rotor, downstream to rotor and exit from the turbine where the empirical loss coefficients will be applied. These are shown in detail in Figs 1 & 2 at meridional view of the turbine with corresponding station numberings. Throughout the remaining of this paper, these stations will be referred as Station 1, 2, 3 and 4 respectively. Details of the mean line model calculations are explained by Romagnoli [4]. The losses taking place at different stations are summarized as in Table 1.

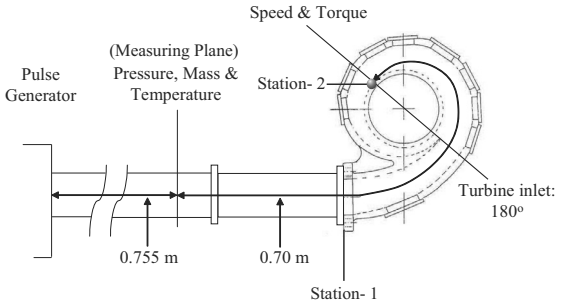

Figure 1: Mean flow path throughout turbine and illustration of turbine Station 1 & 2 [3]

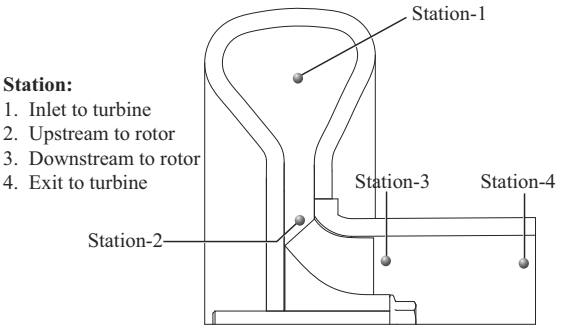

Figure 2: Turbine Station 1, Station 2, Station 3 and Station 4 [4]

Table 1: Losses across stations in mean line model

Station	Losses
1 to 2	Stator pressure drop, entropy gain in flow angular momentum
2 to 3	Incidence loss, passage loss
3 to 4	Clearance loss, disc friction loss

One-dimensional Gas Dynamic Model

One-dimensional gas dynamic model is solved using one-dimensional Navier-Stokes equations, which

are the conservation of continuity, momentum and energy equations. Compared to the mean line model where only the continuity equation is conserved, a gas dynamic model is obviously capable of producing a more realistic prediction result. Another advantage of a gas dynamic model over mean line model is that the governing equations of gas dynamic model are a set of non-linear hyperbolic partial differential equations, as in Eqs. 1 & 2, thus dominated by wave-like phenomena [5]. As a result, it enables a closer study on the wave activity of gas flow in turbine volute or throughout the exhaust pipe system. This is vital for analyzing pulsating flow performance of a turbine at highly unsteady inflow [6].

Several researchers had modeled a turbine one-dimensionally as series of nozzles [7] or represented a turbine rotor as pressure drop boundary [8, 9] and solved using non-homentropic gas dynamic model. The single entry nozzled radial turbine model developed by Serrano et. al. [7] managed a good pressure prediction at turbine inlet and outlet under pulsating flow. Costall et. al. [9] also showed the instantaneous pressure, mass flow rate and mass flow parameter at the measuring plane of twin entry turbine under full and partial pulsating inflow can be predicted by assuming the rotor as a quasi-steady pressure drop boundary. The specific details of the one-dimensional gas dynamic model were explained in Winterbone & Pearson [5] and Costall [8].

However, one of the drawbacks of these turbine models is the lack of efficiency and turbine work computation. Work transfer from a radial turbine is defined by Euler turbomachinery equation (Eq. 3), that is, the change of total enthalpy across a turbine, which in turn related to the change of rotor radius as gas flows from rotor inlet to outlet. In one-dimensional gas dynamic model, turbine is modeled as series of pipe (or nozzle if varying cross-sectional existed) and the effect of radius change and consequently the gas flow velocity change was not included. Another limitation of the current gas dynamic turbine model is the inability of calculating velocity triangle. Velocity triangle is a unique feature found in turbomachines as gas flow cross the boundary between stagnant volute and rotating rotor.

$$\frac{\partial \mathbf{W}}{\partial t} + \frac{\partial \mathbf{F}(\mathbf{W})}{\partial x} + \mathbf{C} \qquad (1)$$

$$where, \qquad \mathbf{W} = \begin{bmatrix} \rho F \\ \rho u F \\ \rho e_0 F \end{bmatrix},$$

$$\mathbf{F}(\mathbf{W}) = \begin{bmatrix} \rho u F \\ (\rho u^2 + P) F \\ \rho u h_0 F \end{bmatrix},$$

$$\mathbf{C} = \begin{bmatrix} 0 \\ -P\frac{df}{dx} \\ 0 \end{bmatrix} + \begin{bmatrix} 0 \\ \rho G F \\ -\rho q F \end{bmatrix} \qquad (2)$$

$$\begin{aligned} \dot{W} &= \dot{m}(h_{0\text{in}} - h_{0\text{out}}) \\ &= \dot{m}(U_{\text{in}} C_{\theta\text{in}} - U_{out} C_{\theta\text{out}}) \end{aligned} \qquad (3)$$

On the other hand, the calculation from station to station in a mean line model does include the velocity triangle effects and losses features that the gas dynamic turbine model is not capable of. The objective of coupling these two computation methods is to counter-balance the associated limitation in their individual methods. In the following sections, the coupling methodology will be discussed in detail and the predicted flow performance and efficiency of a single entry nozzleless mixed flow turbine at 43.0 rps/$\sqrt{K}$ under steady flow and 60 Hz pulsating flow will be compared with testing results.

Experimental Result

The predicted flow performance and turbine efficiency will be compared with available experimental results. The nozzleless mixed flow turbine was previously tested using cold-flow turbocharger test facility at Imperial College at 27.0 to 53.7 rps/$\sqrt{K}$ operating speed. The details of the test rig, testing procedures and experiment results are described in Szymko [3]. The steady state mass flow parameter and turbine efficiency are shown in Fig 3. While turbine mass flow parameter and efficiency at 43.0 rps/$\sqrt{K}$ under 60Hz pulsating flow are illustrated in Fig 4.

METHODOLOGY

Its been discussed previously that the disadvantage of mean line model is the momentum and energy equations are not conserved during computation. In steady flow computation, these do not cause any issue since flow properties are allowed to achieve equilibrium state and mass flow rate at turbine inlet always proportional to the local pressure level. However under pulsating flow, the change in pressure will propagate along the turbine volute in the form of disturbance wave at a much higher speed, which found to be the sum of bulk flow velocity and sonic velocity [3, 6]. Seeing that the mass flow rate only propagate at bulk flow velocity, a larger phase difference may be observed between pressure and mass flow rate profile further downstream to the volute. As the unsteadiness of pulsating flow increases, the deviation becomes more pronounce. The methodology of this paper treated the nozzleless turbine as three distinct portions: volute, rotor and exducer.

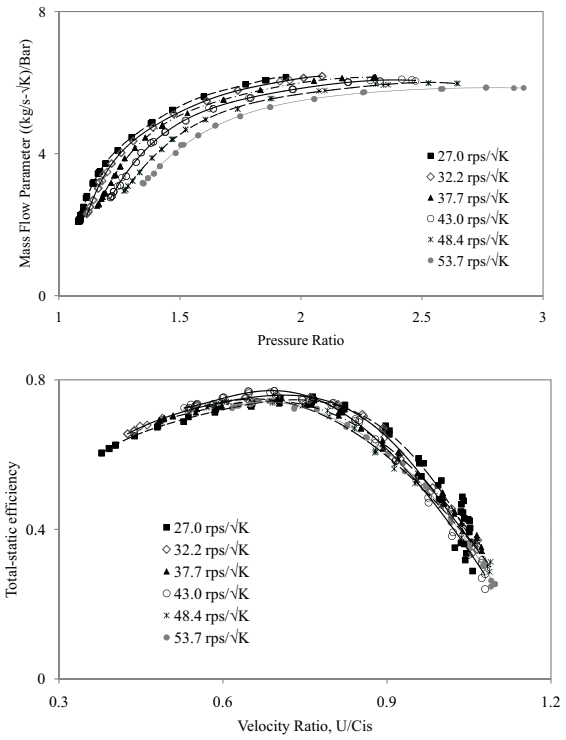

Figure 3: Steady state mass flow parameter and turbine efficiency at 27.0 – 53.7 rps/$\sqrt{K}$ turbine speed [3]

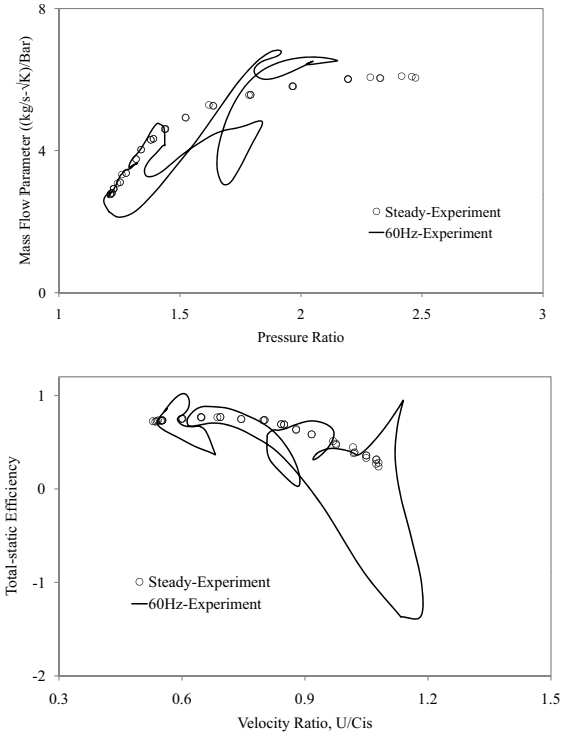

Figure 4: Turbine mass flow parameter and efficiency under 60Hz pulsating flow at 43.0 rps/$\sqrt{K}$ turbine speed [3]

Volute

In a turbine volute (Station- 1 to 2), gas flow is free to move and accelerate. Since no work transfer exist in this portion, it is appropriate to model volute as series of pipes using one-dimensional gas dynamic model. Another important consideration is the higher volute to overall turbine volume ratio. The quasi-steady assumption is valid only if the volume of that particular portion is small compared to the whole system, so that $\frac{\partial \gamma}{\partial t} \gg \frac{\partial \gamma}{\partial x}$, where γ is any flow parameter under consideration. With such a high volute to turbine volume ratio, quasi-steady assumption might not applicable at turbine volute. This was proved in pulsating flow turbine testing where phase shifting of instantaneous flow parameters with different shifting velocity was required before performance parameter can be computed [3, 10].

Rotor

Compared to the volute, the rotor (Station-2 to 3) to overall turbine volume ratio is much lower, and distance of gas flow travel in much shorter as well. Therefore, quasi-steady assumption will be made at rotor portion and mean line model will be used for performance calculation. With this assumption, the instantaneous flow parameters at rotor inlet and outlet will be in phase regardless whether the inflow is pulsating or steady. Since mean line model is utilized, the velocity triangle at rotor inlet and outlet, radius change effect and incidence losses can be considered as well. This is important to compute the turbine efficiency as it allows work transfer calculation.

Exducer

In turbine modeling, the gas flow parameter at exducer (Station- 3 to 4) is important for pressure ratio calculation. In this study, the gas flow in exducer portion will be computed using mean line model assuming that the flow parameters were extracted immediately after the rotor exit. If the flow parameters were extracted further downstream to rotor exit, the effect of phase difference may become significant and calculation using mean line model may no longer accurate.

Modeling

The modeling procedures started by validation with experimental steady-state result and consequently extended to pulsating flow performance analysis. Firstly, turbine volute (Station-1 to 2) was modeled using one-dimensional gas dynamic model so that flow parameters upstream to nominal rotor inlet can be extracted as inputs to the

mean line model for rotor and exducer. The one-dimensional gas dynamic model was developed according to methodology outlined by Costall [8]. The turbine volute was represented by a constant cross-sectional area pipe object of same length and volume. Nominal rotor inlet was located at 180° azimuth angle where all flow was assumed to enter the rotor. Another pipe object, with the length from rotor inlet to exducer was connected immediately downstream to nominal rotor inlet, representing rotor and exducer portion. Two pressure drop boundaries were utilized in turbine model. First pressure drop boundary located upstream to turbine tongue and calibrated to simulate pressure drop across the volute, while the second at nominal rotor inlet, calibrated to simulate pressure drop at rotor. The schematic diagram of the numerical model is shown in Fig 5.

At this stage, it is necessary to model the whole turbine in one-dimensional gas dynamic model due to the flow parameter upstream to nominal rotor inlet is affected by flow condition downstream of it as well. Two conditions that must be fulfilled by turbine model at this point are: (1) Mass flow parameter and pressure ratio across whole turbine stage and (2) Mass flow rate parameter and pressure across volute (up to nominal rotor inlet). These are shown in Fig 6. Predicted mass flow parameter across the turbine was compared to experimental result while predicted mass flow parameter across the volute was compared to those computed using empirical relationship typically utilized in mean line model, considering that mean line model is capable of producing good performance prediction under steady flow.

Flow parameters extracted at nominal rotor inlet are the: total pressure, P_{02}, total temperature, T_{02}, static pressure, P_2, static temperature, T_2 and nominal rotor inlet radial velocity, C_{m2}. These parameters will be used as input to Station 2 in mean line model for turbine efficiency calculation. The predicted gas flow velocity in turbine model at nominal rotor inlet is assumed to be the meridional velocity component into rotor (C_{m2}) in mean line model since it is along the mean flow path of the turbine. At this point, it is necessary to compute the inlet velocity triangle in order to evaluate the remaining losses. Absolute flow angle can be computed from A/r ratio and density change across volute, as shown in Eq. 4. Absolute velocity (C_2), relative velocity (W_2) and tangential velocity component ($C_{\theta 2}$) can be determined from absolute flow angle using trigonometry rules and thus the inlet velocity triangle can be constructed.

Incidence loss occurred when relative flow angle of the gas flow approaching the rotor inlet deviated from rotor blade angle. Incidence loss used in the

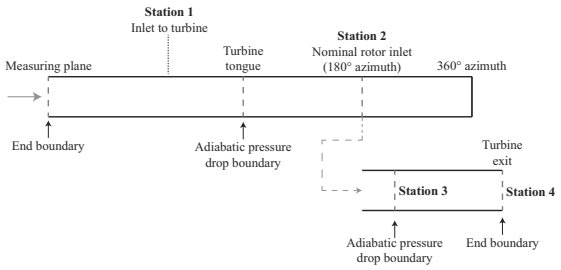

Figure 5: Schematic diagram of the numerical model

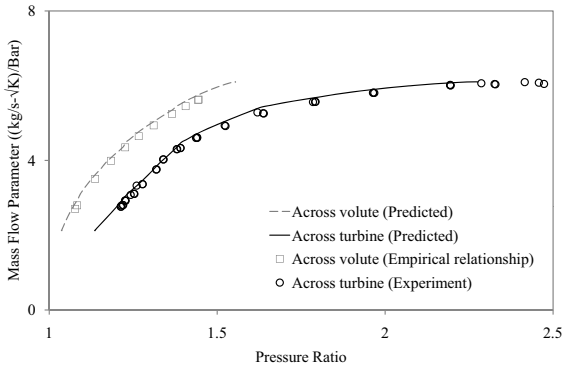

Figure 6: Predicted MFP-PR across stator and turbine

mean line model is shown in Eqs. 5 & 6 [11, 12]. Passage loss is assumed to be proportional to the mean kinetic energy of the gas flow in rotor passage as in Eq. 7 [4]. Clearance loss is expressed as a function of ratio of the tip clearance to exit blade height, shown in Eq. 8. This loss is due to the clearance between shroud and rotating rotor blade tip. Disc friction is caused by viscous friction as air leaked into clearance space between the back plate of rotating rotor and the stationary turbine housing. Disc friction loss is expressed in Eq. 9 [13]. The predicted steady state turbine efficiency is shown in Fig 7 compared with the experimental result, which shows good agreement with experimental result.

$$tan\ \alpha_2 = \frac{\rho_2}{\rho_1} \cdot \frac{A_2/r_2}{A_1/r_1} \tag{4}$$

$$L_{\text{inc}} = K_{\text{cl}} \cdot 0.5[W_2 sin(\beta_2 - \beta_{\text{b2}} - i_{\text{opt}})]^2 \quad (5)$$
$$for |\beta_2 - \beta_{\text{b2}} - i_{\text{opt}}| < \tfrac{\pi}{4}$$

$$L_{\text{inc}} = K_{\text{cl}} \cdot 0.5 W_2^2 [0.5 + |\beta_2 - \beta_{\text{b2}} - i_{\text{opt}}| - \tfrac{\pi}{4}] \quad (6)$$
$$for |\beta_2 - \beta_{\text{b2}} - i_{\text{opt}}| > \tfrac{\pi}{4}$$
$$where, i_{\text{opt}} = tan^{-1}\left(\tfrac{-1.98 tan\ \alpha_2}{Z(1-1.98Z)}\right)$$

$$L_{\text{p}} = K_{\text{p}} \frac{[W_2^2 cos^2(|\beta_2 - i_{\text{opt}}|) + W_3^2]}{2} \tag{7}$$

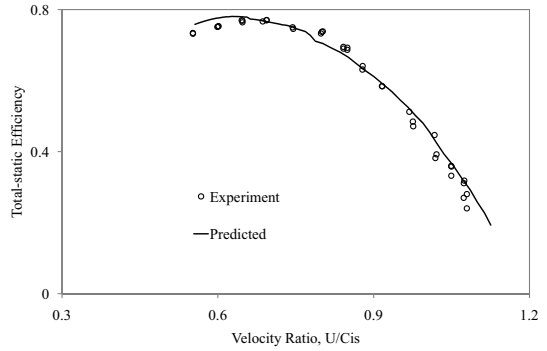

Figure 7: Predicted steady state turbine efficiency

$$L_{\mathrm{cl}} = \frac{2\Delta h_{23}(H_{\mathrm{cl}}/2r_{3,\mathrm{tip}})}{1-(r_{3,\mathrm{hub}}/r_{3,\mathrm{tip}})} \tag{8}$$

$$L_{\mathrm{df}} = \frac{0.02125U_2^2\rho_2^2}{\dot{m}(\rho_2 U_2 r_2/\mu)^{0.2}} \tag{9}$$

Having validated against the experimental steady state performance, the turbine numerical model was used for performance prediction under 60 Hz pulsating flow. Experimental instantaneous total pressure and total temperature were applied as input to the numerical model and the instantaneous inlet mass flow rate was predicted. Flow parameters extracted at nominal rotor inlet were first phase shifted to a common reference plane (measuring plane, refer Fig 1) before the aforementioned efficiency calculation was conducted.

RESULT

The predicted instantaneous static pressure, static temperature and mass flow rate into turbine with 60 Hz pulsating inflow are shown in Figs 8–10. From Figs 8 & 9, the static pressure and temperature was found to follow closely with experimental results except for some under-estimation at 120°–160° pulse cycle. Maximum static pressure and temperature prediction error recorded are 7.8% and 4.4% respectively. Beyond 120° pulse cycle, the estimated pressure and temperature profiles were also found to be marginally lagging behind the experimental result. These deviations were reflected in the predicted mass flow rate profile where larger mass flow rate, which almost twice as much as experimental value was noticed at 120°–160° pulse cycle. This huge difference is mainly due to prediction profile is out of phase with experimental profile at that particular pulse cycle region. In Fig 10, the predicted out-of-phase mass flow peak and valley are showed in relative to the corresponding experimental measured peak and valley.

The predicted mass flow rate shown in Fig 10 was recorded at nominal rotor inlet since this represents the exact amount of instantaneous flow rate into the rotor. The mass flow rate profile was phase shifted to numerical model inlet so that turbine performance can be calculated. The phase difference between the predicted and experimental mass flow rate profile could be caused by the use of constant average phase shifting velocity. Due to varying temperature level in pulsating flow, the local sonic velocity of flow is varying throughout the pulse cycle as well as the gas flow propagation speed. This can be seen in Fig 11 where the predicted mass flow profile is shifted with different shifting velocities. It was found phase shifting using the sum of sonic and bulk flow velocity (denoted as V-shift in Fig 11) matched the mass flow profile of high energy level well while lower shifting velocity (approximately 80-90% of V-shift) is required to match the mass flow rate profile at lower pressure and temperature level. This indicates that a more comprehensive shifting method should be utilized if the entire flow rate profile is to be matched.

However, constant average shifting velocity will be used at this stage of the work since similar method was used to post-process the experimental results. The comparisons between experimental results and the predicted pressure ratio, turbine mass flow parameter, velocity ratio and efficiency when subjected to 60 Hz pulsating flow are illustrated in Fig 12. These results are plotted against pulse cycle to enable a closer look on how each parameter changes with inlet pulsating flow.

Pressure ratio, being calculated from inlet total pressure, closely follows the trend of inlet pressure variation. It can be seen that the pulse features are broadly predicted well. Meanwhile, it can be noticed that error in the mass flow rate prediction at turbine inlet has direct impact to the predicted mass flow parameter. The over-estimation of flow rate and phase difference compared to the experimental result after 120° pulse cycle is clearly visible in the predicted mass flow parameter. Turbine efficiency is a function of the inlet total enthalpy, thus related to inlet flow velocity and mass flow rate. Therefore, the prediction quality of the inlet mass flow rate is also implicitly affecting the efficiency prediction. The resultant swallowing capacity and efficiency curves compared to the experimental results are presented in Fig 13.

Turbine swallowing capacity under pulsating flow was predicted within acceptable pressure ratio range, even though one would notice mismatch at peak pressure ratio. This corresponds to the mismatch in pressure ratio peak in Fig 12. The disparity between experimental and predicted mass flow rate is once again appeared in swallowing capac-

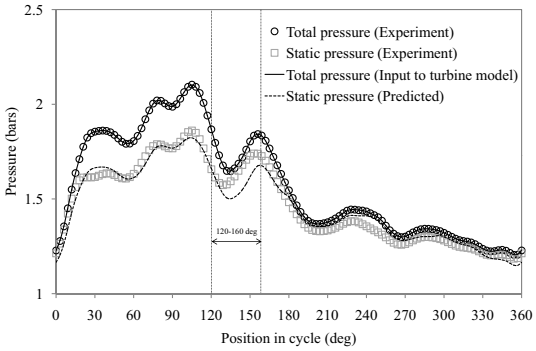

Figure 8: Predicted instantaneous pressure profile under 60 Hz pulsating inflow

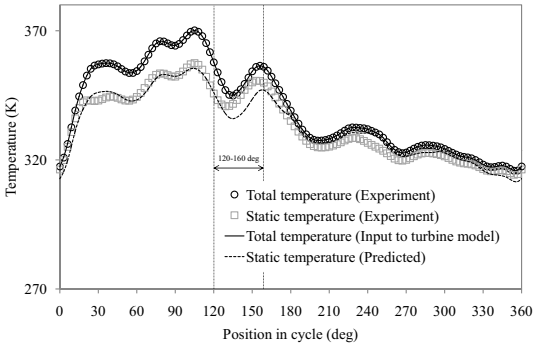

Figure 9: Predicted instantaneous temperature profile under 60 Hz pulsating inflow

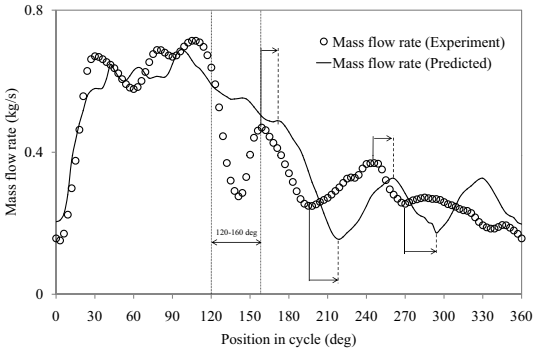

Figure 10: Predicted instantaneous mass flow rate profile under 60 Hz pulsating inflow with illustration of out-of-phase predicted mass flow peak with corresponding experimental peak

ity. The over prediction of mass flow parameter at pressure ratio of 1.6 – 1.9 correspond to higher flow rate predicted at 120°–160° in the pulse cycle (Fig 10). While the highly out-of-phase mass flow rate profile fluctuation at the end of pulse cycle leads to relatively poor prediction of swallowing capacity curve at the low pressure ratio range. Nonetheless, the predicted swallowing capacity curve still fits well inside the maxima and minima of experimental results.

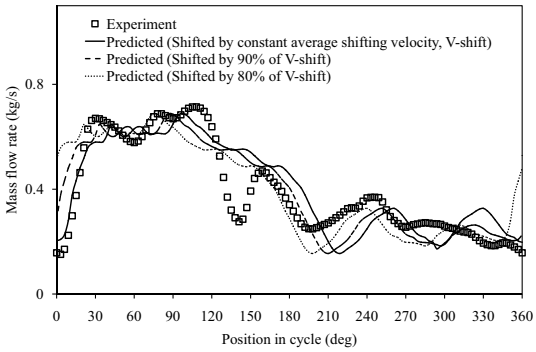

Figure 11: Phase shifting of predicted mass flow rate profile with different shifting velocities

Similarly, efficiency curve was predicted within acceptable velocity ratio range compared to the experimental results. Huge discrepancy in efficiency was observed at high velocity ratio, which is, at extremely low pressure ratio region, where negative efficiency was measured during experimental testing. At medium to low velocity ratio range, efficiency prediction was reasonably good that most of the results fit inside the envelope defined by experimental efficiency curve. The predicted efficiency curve also exhibited consistent deviation as experiment result compared to the steady state efficiency curve. At low velocity ratio range, unsteady turbine efficiency is generally above steady state efficiency whereas at high velocity ratio range, the unsteady efficiency is lower than in steady state.

The actual time duration of a complete 60 Hz pulse is approximately 0.0167s and the exact time interval between two data points in results shown from Figs 8 to 13 is 0.138ms. In reality, it would be almost impractical to 'feel' the change in parameter for every single result point at this rate. Rather what would be more realistically felt by the turbine is an average efficiency and swallowing capacity within the pulse or over a period of time, which is known as isentropic power averaged value [3] shown in Eq. 10. $\gamma_{is,avg}$ in Eq. 10 is any generic parameter to be averaged. Because isentropic power averaged parameter is an average value weighted by instantaneous isentropic power, the instantaneous mass flow rate, pressure ratio and temperature level are taken into account. The percential differences between the experimental and numerical model isentropic power averaged parameters are summarized in Table 2.

Comparison in Table 2 suggested that the developed turbine model enables a satisfactory prediction on isentropic power averaged performance parameters. Isentropic power averaged pressure ratio and velocity ratio are predicted less than 1% of error compared to experimental result. Mass flow param-

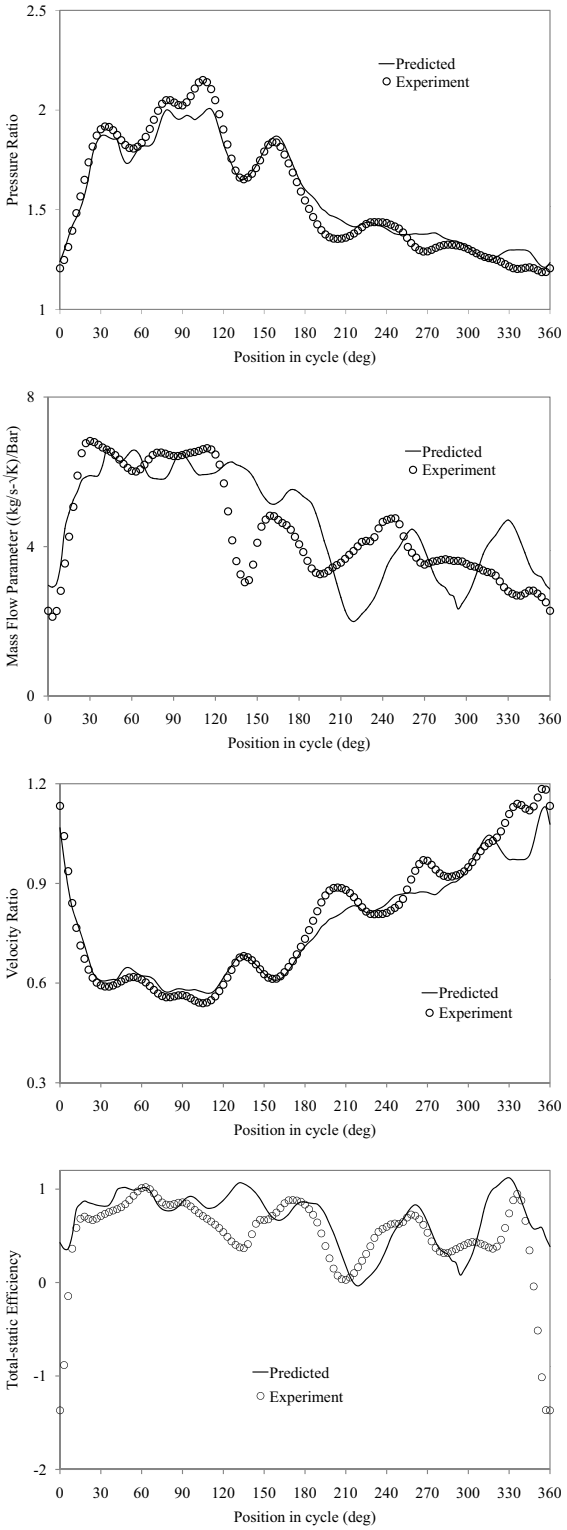

Figure 12: Predicted pressure ratio, mass flow parameter, velocity ratio and efficiency against pulse cycle

eter prediction recorded the highest error (4.25%) compared to experimental result that mainly due to

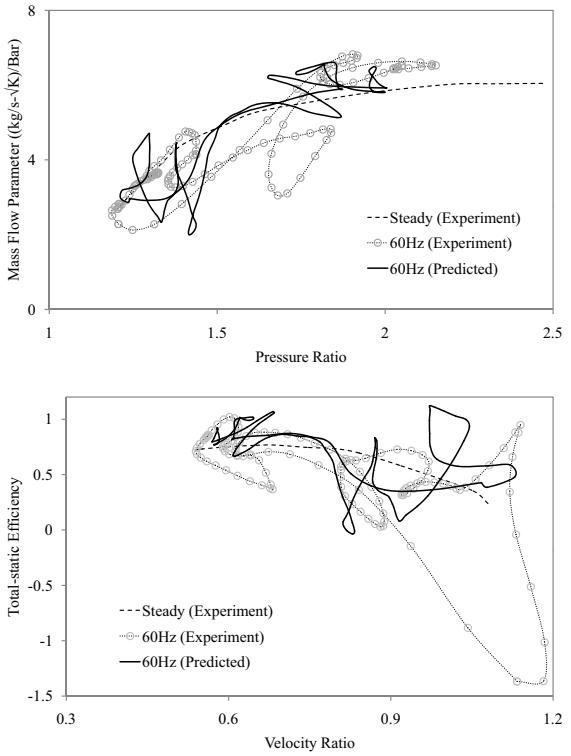

Figure 13: Predicted mass flow parameter-pressure ratio and efficiency-velocity ratio

differences inaccuracy in mass flow rate prediction.

$$\gamma_{is,avg} = \frac{\int_0^\theta \gamma(t) \cdot W_{is}(t)\, dt}{\int_0^\theta W_{is}(t)\, dt} \tag{10}$$

Table 2: Percentage difference of isentropic power averaged parameters between experimental and turbine model

Performance parameter	**Difference [%]**
Pressure ratio	0.12
Mass flow parameter	4.25
Velocity ratio	0.06
Total-static efficiency	2.25

FUTURE DEVELOPMENT

Future development will focus on improving the predictions of the instantaneous mass flow rate at turbine inlet. In addition, the turbine model will also be extended to predict unsteady turbine efficiency at different frequencies of pulsating inflow and at different turbine operating speeds.

SUMMARY OF FINDINGS

A methodology of predicting the turbine swallowing capacity and efficiency under pulsating flow, by coupling one-dimensional gas dynamic model and mean line model had been presented. The methodology was first validated against steady state turbine performance result available from cold flow testing. Having matched the steady state performance, the unsteady turbine swallowing capacity and efficiency curve when subjected to 60 Hz pulsating flow were predicted. The prediction results suggested that instantaneous mass flow rate prediction should be improved in order to obtain better prediction. The pulsating turbine pressure ratio and velocity ratio range were correctly predicted. Turbine efficiency prediction at low velocity ratio (high pressure ratio and high flow energy level regime) was found better than at high velocity ratio. The prediction quality on a broader pespective can be considered good and useful for further analysis. It is known that the instantaneous features of pulsating flow performance are influenced by many factors. These in many ways are experimental limitations in acquiring all the relevant parameters instantaneously, especially the mass flow rate. This has been shown in number of past publications. Thus, an isentropic power averaged comparison is better in assessing the prediction quality. Comparison of isentropic power averaged performance parameters shows satisfactory agreement between the numerical model and the actual testing results.

ACKNOWLEDGEMENTS

The authors would like to thank the Ministry of Higher Education Malaysia and Universiti Teknologi Malaysia for Research University Grant VOT 01J49.

REFERENCES

[1] I. Drescher. Strategies for future powertrains. HOP!, Brussels, June 2008.

[2] J. Pastor. Engine and transmission technology roadmapping: Consequences and opportunities for lubricant and fuels development. 2010 API Automotive/Petroleum Industry Forum, April 2010.

[3] S. Szymko. *The development of an eddy current dynamometer for evaluation of steady and pulsating turbocharger turbine performance*. PhD thesis, Imperial College, University of London, 2006.

[4] A. Romagnoli. *Aerodynamic and thermal characterization of turbocharger turbines: experimental and computational evaluation*. PhD thesis, Imperial College, University of London, June 2010.

[5] D.E. Winterbone and R. J. Pearson. *The Theory of Engine Manifold Design: Wave Action Methods for IC Engines*. Professional Engineering Publishing Ltd, 2000.

[6] S. Szymko, R. F. Martinez-Botas, and K. R. Pullen. Experimental evaluation of turbocharger turbine performance under pulsating flow conditions. In *Proceedings of the ASME Turbo Expo 2005: Power for Land, Sea and Air*, June 2005.

[7] J. R. Serrano, F. J. Arnau, V. Dolz, A. Tiseira, and C. Cervelló. A model of turbocharger radial turbines appropriate to be used in zero- and one-dimensional gas dynamic codes for internal combustion engines modeling. *Energy Conversion and Management*, 49:3729–3745, 2008.

[8] A. Costall. *A one-dimensional study of unsteady wave propagation in turbocharger turbines*. PhD thesis, Imperial College, University of London, September 2007.

[9] A. W. Costall, R. M. McDavid, R. F. Martinez-Botas, and N. C. Baines. Pulse performance modeling of a twin entry turbocharger turbine under full and unequal admission. *Transactions of the ASME, Journal of Turbomachinery*, 133, 2011.

[10] S. Rajoo. *Steady and Pulsating Performance of a Variable Geometry Mixed Flow Turbocharger Turbine*. PhD thesis, Imperial College, University of London, July 2007.

[11] S.M. Futral Jr and C. A. Wasserbauer. Off-design performance prediction with experiment verification for a radial-inflow turbine. Technical Note NASA TN D-2621, National Aeronautics and Space Administration, Washington, D.C., 1965.

[12] N. Mizumachi, D. Yoshiki, and T. A. Endoh. A study on performance of radial turbine under unsteady flow conditions. *Report of the Institute of Industrial Science*, 28:122–130, 1979.

[13] P. L. Meitner and A. J. Glassman. Computer code for off-design performance analysis of radial-inflow turbines with rotor blade sweep. Technical Paper 2199, National Aeronautics and Space Administration, 1983.